2024 10th IEEE RAS/EMBS International Conference for
Biomedical Robotics and Biomechatronics (BioRob)
1-4 September 2024. Heidelberg, Germany

A Novel Personalized Ankle Exoskeleton with Co-Located SEA for Gait Training

Mohamed T. Eraky, Andy Li, Mariana H. Rocha, Aytac Teker, Biruk A. Gebre,
Karen J. Nolan, Kishore Pochiraju, and Damiano Zanotto

***Abstract*— Gait rehabilitation programs help individuals who sustained a brain injury or severe lower-leg trauma realize their full recovery potential. While robotic exoskeletons have emerged as promising tools for gait rehabilitation, high costs and "one-size-fits-all" designs that sacrifice user comfort and fit hinder their wider adoption in clinical settings. In this paper, we present a new modular ankle exoskeleton featuring a personalized Ankle Unit and a portable Actuation Unit. The Ankle Unit is fabricated using affordable additive manufacturing processes to conform to the user's leg morphology. The Actuation Unit, which can be shared across different Ankle Units, utilizes a cable loop to transfer mechanical power to a lightweight, high-stiffness rotary elastic module co-located with the ankle joint. Preliminary treadmill walking tests indicate very good transparency (root mean square error (RMSE) of 0.27 Nm in zero-torque mode) and torque tracking performance (RMSE of 1.16 Nm when applying 10% biomechanical torque assistance, corresponding to a peak commanded torque of 13.7 Nm).**

***Index Terms*— Personalized Ankle Exoskeleton, Robot-Assisted Gait Training, Series Elastic Actuator.**

I. Introduction

Neurological conditions and lower-limb trauma are frequently associated with persistent gait impairments [1]. Task-specific gait training has been shown to promote motor recovery and improve gait function. Given that the ankle plays a crucial role in stabilizing and propelling the body [2], ankle exoskeletons are among the most common lower-limb robotic technologies proposed to enhance or restore ambulatory function through exercise training [3]–[5]. Despite these advances, designing ankle exoskeletons to best promote recovery of walking function remains an open research challenge. In this regard, a key aspect of traditional exercise-based therapy, i.e., the importance of personalizing the interventions to the patient, has been largely overlooked.

The mechanical structure of most ankle exoskeletons is handmade by professional orthotists using plaster molding and thermoplastic vacuum forming, similar to traditional passive orthoses [6]. This process offers limited design options and involves significant labor. Readjustments are often required to improve comfort and fit, but these cannot completely prevent skin abrasions, bruises, pressure sores, and blisters from developing with orthotic use [7]. Since discomfort is the leading cause of low patient compliance with orthotic interventions [8], there is a compelling need for a new design methodology to enable the fabrication of personalized orthoses. This need is even more critical for powered orthoses and exoskeletons, which provide active assistance to the wearer, resulting in larger human-orthosis interaction forces [9].

Fig. 1. Portable ankle exoskeleton Strider for gait training.

Optimizing the weight distribution can also improve comfort in wearable robots [5]. To this end, ankle exoskeletons often rely on cable actuation to remotely transfer mechanical power to the lower leg [3]–[5], [10]. This design solution allows the heaviest components to be worn close to the body's center of mass to reduce the exoskeleton's burden on the user [3], [11]. On the other hand, cable actuation introduces additional frictional forces that are challenging to compensate using feed-forward models alone, making it difficult to accurately estimate the applied ankle torques unless co-located force transducers are used. Bae *et al.* [3] utilized two load cells mounted in-line with the distal ends of the two actuation cables of a soft ankle exosuit. This approach results in added costs and design complexity and requires knowledge of the wearer's anatomical parameters to estimate the ankle interaction torque, which may affect its accuracy

MTE, AL, and DZ (dzanotto@stevens.edu) are with the Wearable Robotic Systems Lab., Stevens Inst. of Technology, Hoboken, NJ 07030, USA.

AT, MHR, BAG, and KP are with the PROOF Lab., Stevens Inst. of Technology, Hoboken, NJ 07030, USA.

KJN is with Human Performance and Engineering Research, Kessler Foundation, West Orange, NJ 07052, USA and Rutgers-NJMS, Newark, NJ 07103, USA.

and ease of applicability. Additionally, while exosuits do naturally conform to the wearer's body, thereby ensuring a good fit, they do not provide the level of mediolateral ankle support that hinged orthoses can afford [12].

Series elastic actuators (SEA) are often used in physical Human-Robot Interaction for their ability to implement "safety by design, performance by control" [13]. Indeed, a system's closed-loop impedance reduces to the SEA passive impedance when external disturbances are beyond the controller bandwidth [14]. In addition, the compliance of SEA improves torque tracking performance by reducing nonlinearities, such as those caused by friction and backlash, in cable-driven wearable robots [14]. The elastic element is a critical component of a SEA, as it determines its range of actuation and torque resolution, and contributes to its closed-loop bandwidth [5]. When the elastic element of a SEA is co-located with the human joint it is designed to assist, interaction torques can be directly estimated from the deformations of its elastic element, thereby providing an accurate and nearly zero-lag reference for the low-level controller. Yet, designing compact and lightweight co-located SEAs for ankle exoskeletons remains a significant challenge given the ankle's high torque demands. Most solutions proposed to date are rather bulky, which may pose obstacles to their routine use by individuals with gait impairments [9], [15], [16]. An alternative solution is to use non-collocated SEAs. Zhong *et al.* [10] introduced a pair of backpack-mounted SEAs for a unilateral cable-driven knee-ankle exoskeleton. While their design improves the exoskeleton's mass distribution on the user body, it does not allow for accurate estimations of the interaction torques due to unmodeled friction forces in the transmission cables. Lee *et al.* [5] proposed a pair of compact hip-pack mounted SEAs for a cable-driven ankle exoskeleton and developed a feed-forward friction compensator informed by the current gait phase. Although their friction compensator can effectively improve the exoskeleton's force tracking performances, it assumes a predefined level of assistance. Moreover, their design requires two motors to actuate a single degree of freedom, a solution shared by other designs [3], [6], which nonetheless is suboptimal for a wearable device where weight is a key design constraint.

In this paper, we introduce a new modular ankle exoskeleton, dubbed Strider (Fig. 1), featuring a personalized Ankle Unit and a backpack Actuation Unit. The Ankle Unit is fabricated using a design workflow that generates a subject-tailored model from 3D scans capturing essential user-specific anatomical parameters. Strider is equipped with a lightweight, high-stiffness rotary elastic module with a large deformation range. The elastic module is co-located with the wearer's ankle and powered by the backpack Actuation Unit via a single cable loop. This solution ensures accurate tracking of interaction torque while keeping a favorable mass distribution, without relying on friction compensators or dedicated load cells. While a similar concept has been recently proposed by Du *et al.* [17], their ankle exoskeleton is designed to provide dorsiflexion assistance only, and therefore their device does not meet the high torque requirements needed to assist the ankle during push-off.

The remainder of this paper is organized as follows: Section II describes the design workflow that generates personalized Ankle Units. Sections III and IV describe Strider's mechatronic design and controller architecture, respectively, while Section V summarizes preliminary results from treadmill walking tests. Lastly, the paper is concluded in Section VI.

II. Personalized Design Workflow

The design workflow is based on an anatomic reference frame and shape/size information obtained from a patient's scan, similar to our previous work [18]. However, unlike the previous workflow, the parts are decomposed based on ease of assembly/disassembly, constraints from 3D printers, and the polynomial parameterization of key geometric dimensions. The geometric parameterization creates a low-dimensional design space with fewer than ten parameters, enabling considerable shaping and sizing flexibility. This low-dimensional space also adds the additional functionality of varying the thickness axially and the offset distances from the leg, tailoring the stiffness and fit comfort. Moreover, the workflow is automated, allowing consistent design choices across all subjects.

1) Shank Bracket Design: The algorithm calls five tools to process the data collected at the scanning step and constructs the shank bracket design (Fig. 2). Each tool is modular, allowing independent use. The algorithm can be executed from a Graphical User Interface (GUI), offering an accessible way for loading the data, identifying references on new points, and creating new designs. The input of the pipeline is a point cloud representing the scanned surface of the wearer's leg. The algorithm is written in Python and uses Open3D.

The first tool (*Markers Detector*) identifies key references. It receives a point cloud file as an input and returns the center and radii for each of the four reflective markers located at bony landmarks (medial/lateral femoral condyles and malleoli) to identify knee and ankle anatomical axes. To this end, the point cloud is first divided into 4 sub-pointclouds after finding midpoints between the vertices of the original bounding box. Subsequently, the new bounding boxes, each containing one marker, are processed using the Random Sample Consensus (RANSAC) [19] algorithm to

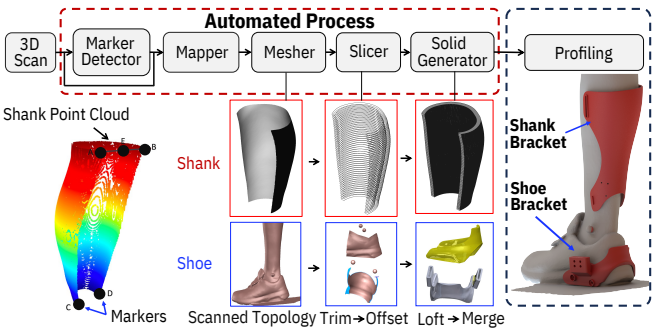

Fig. 2. Proposed automated process to generate personalized shank and shoe brackets from a 3D point cloud.

find clusters in the data selected by the user through a point-picker application. Then, the algorithm fits a sphere to the data in the cluster.

The second tool (*Mapper*) receives an array of coordinates representing the center of the detected markers and the point-cloud as inputs. The output is a point cloud containing the points that represent the surface on the calf. The references are the center of the markers detected using the first tool, and can be selected from a dropwdown menu in the GUI. These references define new axes and keypoints for the shank bracket design. The points from the pointcloud whose height lies between the height of the top and bottom markers (i.e., points A, B, C, and D in Fig. 2) are kept. The pointcloud is then split into posterior and anterior volumes by defining a plane that passes through the midpoint between the top markers (point E) and the ankle markers (points C, D).

The third tool (*Mesher*) uses the Poisson Reconstruction algorithm [20] to interpolate the surface of the split point-cloud, returning a triangle mesh file as output. The Poisson reconstruction algorithm, a spatially adaptive multiscale algorithm, constructs a series of approximations for the mesh of a solid represented by a point cloud. This algorithm builds a globally smooth surface that best fits the segment of the point cloud from the wearer's calf.

Since the output of the previous step is a surface, its topological representation is a 2D manifold. To build a 3D solid, the fourth tool (*Slicer*) receives the mesh from step 3 and slices it using a set of planes orthogonal to the shank longitudinal axis, obtaining a set of curves that discretize the surface. Each curve contains the points that represent the contour of the user's shank at a certain height. New points are created by finding the centroid of the curve and extrapolating the new points in the direction of the centroid-data vector by a predefined thickness value. This thickness value is constrained by two factors: stiffness/strength, and kinematic constrains. The desired stiffness and strength define the minimal amount of material for the shank bracket to be strong but comfortable to wear. The kinematic constraint refer to the coupling between the shank and shoe brackets. The new points surround and close the original curve, allowing the creation of one face per slice.

The fifth and last tool (*Solid Generator*) builds a solid by connecting the points on the contours and constructing triangles in-between. After reading the points in the faces, triangles are created to bind adjacent faces, hence obtaining a 3D object that is exported as a mesh file for printing.

2) Shoe Bracket Design: The shoe bracket is designed following a similar process as described in Sec. II-.1. First, the leg scan is trimmed to the section of interest containing the shoe. An offset surface is created from the shoe, with 1 mm offset. The surface is then thickened to create a solid, and trimmed to an aesthetic profile design. To control the exterior shape of the shoe bracket, the solid is sliced into multiple profiles, a spline tool is used to create splines, and these splines are lofted together to obtain the final design (Fig. 2).

III. System Description

Strider comprises a personalized Ankle Unit, an Actuation Unit fitted on a protective back shield, and a custom-built Li-ion battery anchored on a waist belt. Mechanical power is transmitted from the Actuation Unit to the wearer's ankle through a novel bi-directional torsional rotary SEA, whose elastic module is co-located with the user's ankle joint (Fig. 3), via a Bowden cable loop. Assistive torques from the SEA are transmitted to the user's ankle via a custom bracket attached to the shoe using screws. Unlike ankle exoskeleton designs based on shoe inserts, this solution leverages the shoe's padding to improve user comfort. The weight of the Ankle Unit is 0.8 kg. The heaviest components (5.2 kg Actuation Unit, 1.2 kg Li-ion battery) are located near the body's center of mass to reduce undesired effects of the device's inertia on the wearer's natural gait. In the following sections, the mechatronic design of the Strider exoskeleton is described in detail.

A. Ankle Unit

The Ankle Unit, illustrated in Fig. 3, comprises a personalized shank fabricated from Carbon fiber-PLA (CF-PLA) utilizing FDM 3D printing technology. This shank is constructed ad-hoc, following the workflow described in Sec. II-.1. A 3-mm soft foam layer, contoured to match the inner curvature of the shank using laser cut technology, is positioned as a cushioning interface between the shank module and the wearer's skin. This layer can be easily removed and washed to maintain cleanness and hygiene. The shank is secured to the wearer's shinbone using a wide Velcro strap to ensure comfort. The shank also provides anchoring points for the Bowden cables (AISI 304, 1mm diameter) operating the SEA elastic element. The SEA output shaft is connected to a torque-link, which attaches to the lateral side of the personalized shoe bracket (Sec. II-.2).

The elastic module of the SEA comprises a set of linear compression springs arranged in an arc formation (Fig. 4). This configuration provides a constant stiffness across a wide deformation range. The springs are mounted on two output rotors and seated within the chambers of an input rotor. When the input rotor is rotated by the inner cable of the Bowden Cable, it deflects the springs, generating a reaction torque on the output rotors, which are rigidly connected to each other. The torque generated on the output rotors is transmitted to the torque link using three barrel screws. A miniature optical encoder (E16, US Digital, USA) with 16384 PPR measures the deformation of the elastic element, thereby providing torque feedback for the closed-loop torque controller (Sec. IV-A). A second position sensor (NP24HS-1kΩ, P3 America, Inc., USA) is connected to the medial side of the ankle bracket to measure the ankle plantar- and dorsiflexion angle. The shoe is instrumented with a Force Sensing Resistor (HD 001, IEE S.A., Luxembourg) underneath the heel to detect initial contacts.

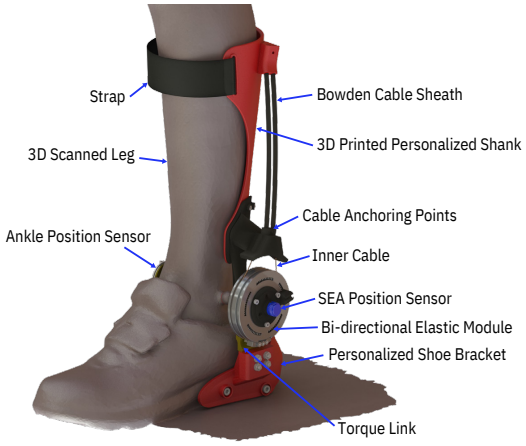

Fig. 3. Rendered view of the Strider Ankle Unit assembly. Bidirectional assistance is achieved via a single cable loop attached to an elastic module co-located with the ankle joint. Personalized shank and shoe brackets are highlighted in red.

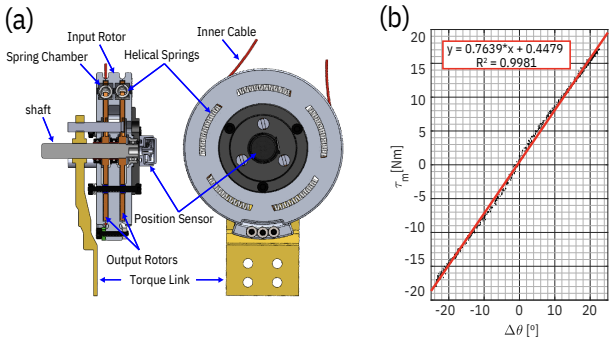

Fig. 4. (a) Sectional (left) and front (right) views showing the main components of the Bidirectional Elastic Module. (b) Passive response of the Elastic Module, demonstrating a constant passive stiffness of 43 Nm/rad (0.764 Nm/deg) across a deformation range of ±24deg.

B. Actuation Unit

The Actuation Unit (Fig. 5) features a backpack-like enclosure (260 mm high, 134 mm thick, 230 mm max width), which is fitted on an articulated protective shield (Ridbiker, USA) and can be used to power either left- or right-side Ankle Units. It includes a brushless motor (EC-90-flat, 600 W, Maxon Group, Switzerland), with integrated encoder (Maxon Mile Encoder 4096 CPT), a motor driver (Maxon EPOS4 Compact 50/15), a Unit Real Time Target Machine (Speedgoat GmbH, Switzerland), and a custom-made data acquisition and conditioning (DAQ) board that features a 32-bit microcontroller (Teensy 3.5, PJRC, USA), an EtherCAT shield (EasyCAT Pro, AB&T Srl, Italy) and a 12-bit ADC (AD7890ANZ-10, Analog Devices, USA). The Real Time Target Machine, the motor driver, and the DAQ communicate over EtherCAT bus. The motor output shaft is connected to a threaded spool (effective diameter: 12.4 mm) to allow for cable winding/unwinding without overlapping. Needle roller bearing cable aligners keep cables within pulley grooves. A cable tensioner ensures positive tension on the unloaded side of the cable during alternating dynamic loads.

The Elastic Module of the SEA has an effective diameter of 76.6 mm, thereby generating a transmission ratio of

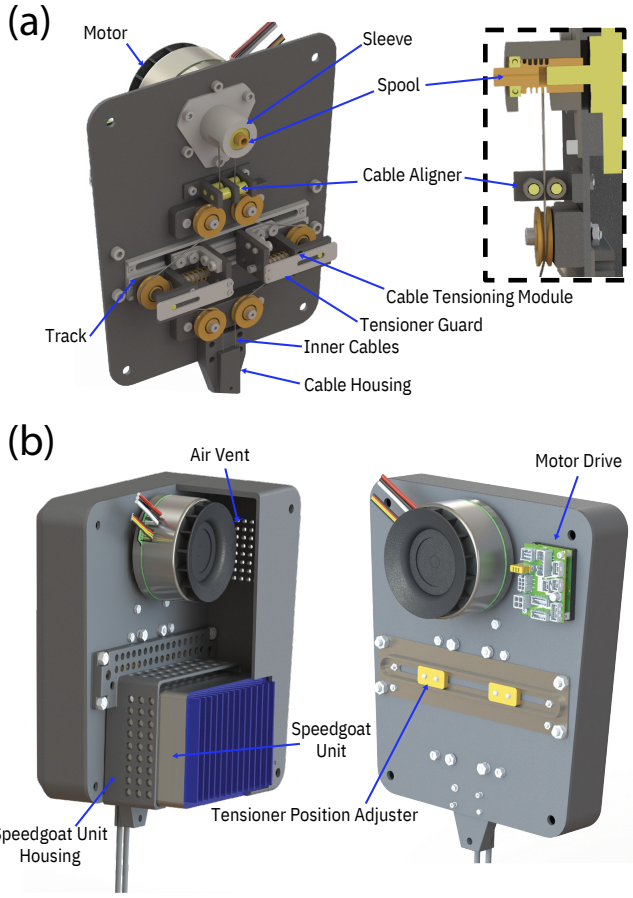

Fig. 5. Rendered view of the Actuation Unit. (a) Front view showing the cable tensioner module and motor spool to wrap and unwrap the cable without overlapping. A cable aligner is used to align cables with pulleys' grooves. (b) Actuation Unit rear view.

approximately 6:1. The maximum assistive torque provided by the exoskeleton is 18 Nm, which corresponds to approximately 15% of the peak ankle plantarflexion torque for a 75 kg adult male walking at normal pace [2]. Notably, this is achieved without the use of a gearbox, thus making the ankle exoskeleton backdriveable.

C. Li-ion Battery

A custom Li-ion battery is designed with a peak current of 30 A, a nominal voltage of 29.4 V (close to the motor's nominal voltage), and capacity of 7000 mAh. The battery is made of a custom assembly of SANYO Li-ion Batteries (NCR18650GA, Sanyo Electric Co., Ltd., Japan) with on-board battery management system and voltage indicator.

IV. Control Architecture

A. Low-level Controller

As shown in Fig. 6, Strider utilizes a cascaded velocity-torque controller whereby a PI compensator in the outer loop (PI_{Torque}) generates the reference velocity ω_d for an inner-loop PI compensator ($PI_{Velocity}$) [21]. The SEA deformation θ_m is used to estimate the interaction torque τ_m. By adopting a high-resolution miniature encoder (Sec. III-B), the SEA can measure angular deformations as small as 0.02°, corresponding to approximately 16.8 mNm (Fig. 4). The gains

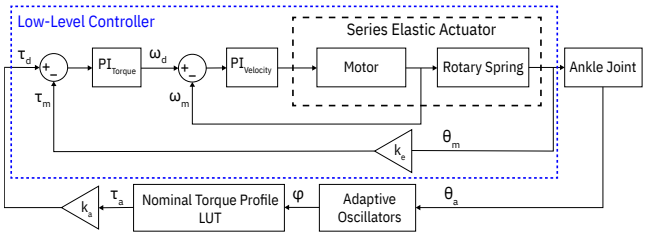

Fig. 6. Strider's low-level controller comprises a cascaded torque-velocity architecture whereby the outer-loop compensator $\mathrm{PI}_{\mathrm{torque}}$ generates the reference velocity ω_{d} for the inner-loop compensator $\mathrm{PI}_{\mathrm{velocity}}$ based on the torque tracking error $(\tau_{\mathrm{d}} - \tau_{\mathrm{m}})$. Strider's assistive controller uses a pool of adaptive frequency oscillators to estimate the current gait phase φ from the measured ankle angle θ_{α}. The desired torque τ_{d} is obtained by scaling the normative ankle torque τ_{a} obtained from a lookup table (LUT) by a predefined factor $\mathrm{k_a}$.

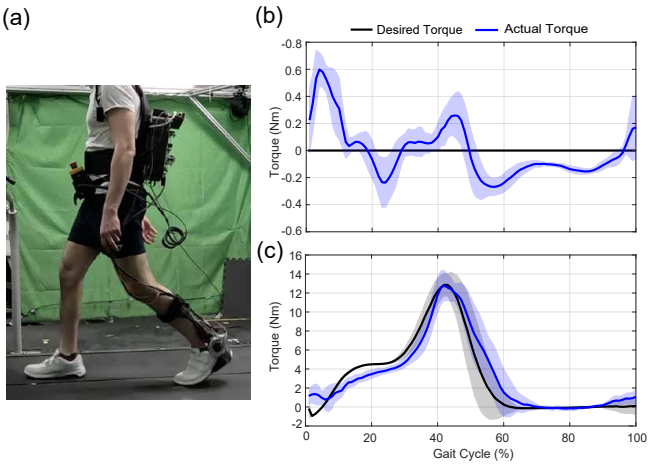

Fig. 7. Performance Evaluation: (a) Healthy subject walking on a treadmill at 0.8 m/s, with the Strider exoskeleton fitted to his left leg. Two trials were performed: zero-torque controller (b), and assistive controller at 10% assistance (c). Solid lines indicate average measured (blue) and commanded (black) torques collected over a 30-second window. Shaded areas indicate ± 1 SD.

for the inner loop velocity controller are auto-tuned using EPOS Studio v3.7, whereas the outer loop gains are tuned manually. The sample rate of the low-level controller is 1 kHz.

B. Preliminary Assistive Controller

A simple assistive controller was implemented for early testing, based on a fixed torque profile, similar to [22]. In this controller, the current ankle angle is fed to a pool of six adaptive frequency oscillators, which continuously estimate the phase of the gait cycle [23]–[25]. The output of the oscillators is aligned with the wearer's initial contacts using the readings from the force sensitive resistor [26], and fed to a lookup table that stores the normative ankle biomechanical moment (Winter's data [2]) as a function of the gait phase. The output of the lookup table is then scaled by a fixed gain to obtain the commanded torque, as shown in Fig. 6.

V. Performance Evaluation

To test Strider's performance, an able-bodied individual (24 year old male, 180 cm height, 78 kg weight) walked on a treadmill (Fig. 7-a) at his comfortable walking speed (0.8 m/s), first in zero-torque mode (i.e., $\tau_{\mathrm{d}} \equiv 0$ Nm), then with 10% assistance (i.e., $\mathrm{k_a} = 0.1$). When the exoskeleton was controlled in zero-torque mode, the root mean square error (RMSE) was 0.20 Nm (Fig. 7-b). When Strider was controlled in assistive mode, the RMSE reached 1.16 Nm (Fig. 7-c). These values correspond to 0.15% and 0.87% of the expected maximum biological ankle moment for normal-pace walking, respectively [2].

VI. Discussion and Conclusion

In this paper, we introduced a personalized cable-driven exoskeleton (Strider) designed to provide bidirectional ankle assistance to individuals with walking impairments during exercise therapy. The exoskeleton leverages a new design workflow that automates the creation of personalized Ankle Units from a 3D scan of the user's lower leg. To reduce the exoskeleton's burden on the user while ensuring accurate torque tracking, the proposed design features a single, non-collocated backdriveable actuator and a co-located SEA elastic module. The Ankle Unit weights 0.8 kg, including the series elastic module (0.2 kg), and can exert up to 18 Nm at the user's ankle. This is in line with the 0.7 kg weight of the design recently presented in [17], which nonetheless can only apply up to 12.5 Nm at the ankle, and outperforms the weight (2.85 kg) of the ankle exoskeleton introduced in [15], which however features a highly geared, co-located actuator. Notably, Strider's maximal torque assistance also exceeds the 14 Nm limit reported in [27], despite not relying on gearboxes. Compared with the ankle exoskeleton presented in [28], which showcases an impressive 30 Nm peak torque at the ankle and a low distal mass of 0.415 kg per leg, the Strider's Ankle Unit is heavier but results in better torque tracking (i.e., RMSE of 1.16 Nm when the peak commanded torque was 13.7 Nm, as shown in Fig. 7-c, vs. 2.25–3.41 Nm reported in [28]). This is achieved by eliminating the gearbox and integrating a co-located SEA.

Strider's SEA design guarantees very good closed-loop transparency. While the peak interaction torque during walking at 0.8 m/s was 0.75 Nm, which seemingly exceeds the 0.28 Nm peak reported by Zhong *et al.* [27], their zero-torque response was measured at the proximal end of the Bowden cables, thereby neglecting the mechanical impedance of the cable transmission. Strider's SEA leverages affordable off-the-shelf springs in a compact parallel arrangement that ensures excellent linearity. This is in contrast to other SEA designs utilizing off-the-shelf parts [17], [29], which obtained highly non-linear responses that may limit the SEA stability region [30] and require the implementation of iterative numerical methods in the low-level control loop.

Current efforts are directed toward evaluating the benefits of the personalized design workflow in terms of comfort and fit, thorough tests with able-bodied individuals and those with motor impairments, using both subjective and objective metrics. Concurrently, a new adaptive controller is being developed to enable robot-assisted over-ground walking exercises.

ACKNOWLEDGMENT

The authors would like to thank R. Deepak, R. Loghmani, P. Stamas, I. Geller, S. Sowrirajan, and M. Parikh for their assistance with CAD modeling, prototyping, and fabrication. The authors also acknowledge the contributions of machinists B. Fraser and P. McClelland who helped with fabrication. This work was supported by the U.S. National Science Foundation under Grant CMMI-1944203 and by the US Department of Defense, through the Peer Reviewed Orthopaedic Research Program (PRORP), under Award No. W81XWH-22-1-0193. Opinions, interpretations, conclusions and recommendations are those of the author and are not necessarily endorsed by the US Department of Defense.

REFERENCES

[1] B. K. Potter, R. G. Sheu, D. Stinner, J. Fergason, J. R. Hsu, K. Kuhn, J. G. Owens, J. Rivera, S. B. Shawen, J. M. Wilken, J. DeSanto, Y. Huang, D. O. Scharfstein, E. J. MacKenzie, and on behalf of the METRC PRIORITI-MTF Team, "Multisite Evaluation of a Custom Energy-Storing Carbon Fiber Orthosis for Patients with Residual Disability After Lower-Limb Trauma," *J. Bone Joint Surg.*, vol. 100, no. 20, pp. 1781–1789, Oct. 2018.

[2] D. A. Winter, *Biomechanics and motor control of human gait*. Waterloo, Ontario: Univ. of Waterloo Press, 1991.

[3] J. Bae, C. Siviy, M. Rouleau, N. Menard, K. O'Donnell, I. Geliana, M. Athanassiu, D. Ryan, C. Bibeau, L. Sloot *et al.*, "A lightweight and efficient portable soft exosuit for paretic ankle assistance in walking after stroke," in *2018 IEEE international conference on robotics and automation (ICRA)*. IEEE, 2018, pp. 2820–2827.

[4] D. Kobsar, J. M. Charlton, C. T. Tse, J.-F. Esculier, A. Graffos, N. M. Krowchuk, D. Thatcher, and M. A. Hunt, "Validity and reliability of wearable inertial sensors in healthy adult walking: A systematic review and meta-analysis," *J. Neuroeng. Rehabil.*, vol. 17, pp. 1–21, 2020.

[5] S. Lee, S. Choi, C. Ko, T. Kim, and K. Kong, "Design and control of the compact cable-driven series elastic actuator module in soft wearable robot for ankle assistance," *Int. J. Control Autom. Syst.*, vol. 21, no. 5, pp. 1624–1633, 2023.

[6] Y. Zhang, R. J. Kleinmann, K. J. Nolan, and D. Zanotto, "Preliminary validation of a cable-driven powered ankle–foot orthosis with dual actuation mode," *IEEE Trans. Med. Robot. Bionics*, vol. 1, no. 1, pp. 30–37, 2019.

[7] B. Menger, A. Kannenberg, W. Petersen, T. Zantop, I. Rembitzki, and H. Stinus, "Effects of a novel foot–ankle orthosis in the non-operative treatment of unicompartmental knee osteoarthritis," *Arch. Orthop. Trauma Surg.*, vol. 136, pp. 1281–1287, 2016.

[8] E. Swinnen, N. Lefeber, A. Werbrouck, Y. Gesthuizen, L. Ceulemans, S. Christiaens, L. De Wael, R. Buyl, S. Ilsbroukx, J. Van Nieuwenhoven *et al.*, "Male and female opinions about orthotic devices of the lower limb: A multicentre, observational study in patients with central neurological movement disorders," *NeuroRehabilitation*, vol. 42, no. 1, pp. 121–130, 2018.

[9] K. Langlois, M. Moltedo, T. Bacek, C. Rodriguez-Guerrero, B. Vanderborght, and D. Lefeber, "Design and development of customized physical interfaces to reduce relative motion between the user and a powered ankle foot exoskeleton," in *2018 7th IEEE International Conference on Biomedical Robotics and Biomechatronics (Biorob)*, 2018, pp. 1083–1088.

[10] B. Zhong, M. Shen, H. Liu, Y. Zhao, Q. Qian, W. Wang, H. Yu, and M. Zhang, "A cable-driven exoskeleton with personalized assistance improves the gait metrics of people in subacute stroke," *IEEE Trans. Neural Syst. Rehabil. Eng.*, 2023.

[11] G. M. Gasparri, J. Luque, and Z. F. Lerner, "Proportional joint-moment control for instantaneously adaptive ankle exoskeleton assistance," *IEEE Trans. Neural Syst. Rehabil. Eng.*, vol. 27, no. 4, pp. 751–759, 2019.

[12] J. C.-M. Fu, Y.-J. Chen, C.-F. Li, Y.-H. Hsiao, and C.-H. Chen, "The effect of three dimensional printing hinged ankle foot orthosis for equinovarus control in stroke patients," *Clinical Biomechanics*, vol. 94, p. 105622, 2022.

[13] A. Albu-Schäffer, A. Bicchi, G. Boccadamo, R. Chatila, A. De Luca, A. De Santis, G. Giralt, G. Hirzinger, V. Lippiello, R. Matone *et al.*, "Physical human-robot interaction in anthropic domains: safety and dependability," in *Proceeding 4th IARP/IEEE-EURON Workshop on Technical Challenges for Dependable Robots in Human Environments*, 2005.

[14] G. Carpino, D. Accoto, F. Sergi, N. Luigi Tagliamonte, and E. Guglielmelli, "A novel compact torsional spring for series elastic actuators for assistive wearable robots," *J. Mech. Design*, vol. 134, no. 12, p. 121002, 2012.

[15] B. DeBoer, A. Hosseini, and C. Rossa, "A discrete non-linear series elastic actuator for active ankle-foot orthoses," *IEEE Robot. Autom. Lett.*, vol. 7, no. 3, pp. 6211–6217, 2022.

[16] F. De Gaitani, W. dos Santos, and A. A. G. Siqueira, "Design and performance analysis of a compact series elastic actuator for exoskeletons," *J. Control. Autom. Electr. Syst.*, vol. 33, no. 3, pp. 1012–1021, 2022.

[17] H. Du, W. Jiang, Y. Qian, W. Zhuang, Y. Guo, Y. Leng, and C. Fu, "A lightweight ankle exoskeleton driven by series elastic actuator," in *International Conference on Intelligent Robotics and Applications*. Springer, 2023, pp. 145–153.

[18] B. A. Gebre, R. Nogueira, S. Patidar, R. Belle-Isle, K. Nolan, K. Pochiraju, and D. Zanotto, "Efficient digital modeling and fabrication workflow for individualized ankle exoskeletons," in *ASME International Mechanical Engineering Congress and Exposition*, vol. 85598. American Society of Mechanical Engineers, 2021, p. V005T05A068.

[19] M. A. Fischler and R. C. Bolles, "Random sample consensus: a paradigm for model fitting with applications to image analysis and automated cartography," *Commun. ACM*, vol. 24, no. 6, pp. 381–395, 1981.

[20] M. Kazhdan, M. Bolitho, and H. Hoppe, "Poisson surface reconstruction."

[21] H. Vallery, J. Veneman, E. Van Asseldonk, R. Ekkelenkamp, M. Buss, and H. Van Der Kooij, "Compliant actuation of rehabilitation robots," *IEEE Robot. Autom. Mag.*, vol. 15, no. 3, pp. 60–69, 2008.

[22] T. Lenzi, M. C. Carrozza, and S. K. Agrawal, "Powered hip exoskeletons can reduce the user's hip and ankle muscle activations during walking," *IEEE Transactions on Neural Systems and Rehabilitation Engineering*, vol. 21, no. 6, pp. 938–948, 2013.

[23] Y. Zhang, K. J. Nolan, and D. Zanotto, "Oscillator-based transparent control of an active/semiactive ankle-foot orthosis," *IEEE Robotics and Automation Letters*, vol. 4, no. 2, pp. 247–253, 2018.

[24] Y. Zhang, S. Li, K. J. Nolan, and D. Zanotto, "Reinforcement learning assist-as-needed control for robot assisted gait training," in *2020 8th IEEE RAS/EMBS International Conference for Biomedical Robotics and Biomechatronics (BioRob)*. IEEE, 2020, pp. 785–790.

[25] ——, "Shaping individualized impedance landscapes for gait training via reinforcement learning," *IEEE Transactions on Medical Robotics and Bionics*, vol. 4, no. 1, pp. 194–205, 2021.

[26] T. Yan, A. Parri, V. Ruiz Garate, M. Cempini, R. Ronsse, and N. Vitiello, "An oscillator-based smooth real-time estimate of gait phase for wearable robotics," *Autonomous Robots*, vol. 41, pp. 759–774, 2017.

[27] B. Zhong, K. Guo, H. Yu, and M. Zhang, "Toward gait symmetry enhancement via a cable-driven exoskeleton powered by series elastic actuators," *IEEE Robot. Autom. Lett.*, vol. 7, no. 2, pp. 786–793, 2021.

[28] G. Orekhov, Y. Fang, C. F. Cuddeback, and Z. F. Lerner, "Usability and performance validation of an ultra-lightweight and versatile untethered robotic ankle exoskeleton," *J. Neuroeng. Rehabilitation.*, vol. 18, no. 1, p. 163, Nov. 2021.

[29] Y. Qian, S. Han, Y. Wang, H. Yu, and C. Fu, "Toward improving actuation transparency and safety of a hip exoskeleton with a novel nonlinear series elastic actuator," *IEEE/ASME Trans. Mechatron.*, vol. 28, no. 1, pp. 417–428, 2022.

[30] L. Sun, M. Li, M. Wang, W. Yin, N. Sun, and J. Liu, "Continuous finite-time output torque control approach for series elastic actuator," *Mech. Syst. Signal Process.*, vol. 139, p. 105853, 2020.